

Elastodynamic antiplane deformation of a bimaterial with an imperfect viscoelastic interface: a dual reciprocity hypersingular boundary integral solution

Whye-Teong Ang

Division of Engineering Mechanics

School of Mechanical and Aerospace Engineering

Nanyang Technological University

50 Nanyang Avenue, Singapore 639798

E-mail: mwtang@ntu.edu.sg

<http://www.ntu.edu.sg/home/mwtang/>

Abstract

A boundary element method based on a hypersingular integral and dual-reciprocity formulation is proposed for the numerical solution of a dynamic antiplane problem involving an elastic bimaterial with an imperfect viscoelastic interface. The interface is modelled using linear springs and dashpots with a jump in the interfacial displacement. To reduce the problem approximately to a system of linear algebraic equations, the Laplace transform is employed to suppress the time derivatives of the unknown functions. Once the linear algebraic equations are solved, the physical solution is recovered through the use of a numerical method for inverting Laplace transform. The proposed method is applied to solve some specific problems.

Preprint. This article has been accepted for publication in *Applied Mathematical Modelling* 31 (2007) 749-769. For more details, please visit

<http://dx.doi.org/10.1016/j.apm.2005.12.007>

1 Introduction

Composites consisting of two or more dissimilar materials play an important role in modern technology. For example, media with a large number of very fine layers are employed in optical recording, and synthetic materials, such as plywood and fabric laminates, are widely used in the design and construction of modern aircrafts. Many studies assume the dissimilar materials are perfectly joined to one another along their common boundaries (see, for example, Ang [1], Berger and Karageorghis [2], Clements [3] and Lee and Kim [4]). In reality, microscopic imperfections are bound to be present along the interfaces of the materials. Because of this, in recent years, there is a surging interest in the analyses and the modelling of microscopically imperfect interfaces (see, for example, Benveniste and Miloh [5], Fan and Sze [6], Ang *et al.* [7] and other references therein).

The numerical solution of an antiplane problem involving an elastic bimaterial with a plane interface that is microscopically imperfect and viscoelastic is considered here. As in Fan and Wang [8], the interface is modelled using linear springs and dashpots with a jump in the interfacial displacement. The model has practical applications in engineering. For example, such an imperfect viscoelastic interface may be observed at room temperature (that is, at around 300° Kelvin) when epoxy with a melting temperature between 340° and 380° Kelvin is used as an adhesive to join together a pair of metals with a high melting temperature (for example, aluminium with a melting temperature of about 1000° Kelvin).

Ang and Fan [9] describes a hypersingular boundary integral method for solving the problem. In their work, the antiplane deformation of the bimaterial is taken to be in a quasi-static state with the antiplane displacement governed by the two-dimensional Laplace's equation, that is, the acceleration term in the governing partial differential equation is assumed negli-

gible. The present paper considers the full dynamic problem by retaining the acceleration term, so that the antiplane deformation is governed by the two-dimensional wave equation.

As in [9], the Green's function for the corresponding perfect interface in an elastostatically deformed bimaterial is used to obtain a hypersingular boundary integral formulation for the problem under consideration. Such a Green's function is a modified fundamental solution of the two-dimensional Laplace's equation and it is relatively simple to evaluate as its terms involve only the elementary logarithmic function. An undesirable consequence of using such an elastostatic modified fundamental solution for an elastodynamic problem is that the acceleration term in the wave equation gives rise to additional integrals over the entire physical domain of the bimaterial. However, as shown in Brebbia and Nardini [10], Partridge and Brebbia [11] and many other papers in the literature, the domain integral may be successfully treated without having to discretise the solution domain into tiny cells or elements. An alternative approach would be to use the fundamental solution for the modified Helmholtz equation (see, for example, Rizzo and Shippy [12]), but this would require a greater computational effort in computing the modified Bessel function and its derivative and the kernel of the hypersingular integral in the formulation of the imperfect viscoelastic interface would assume a more complicated form.

A boundary element procedure together with the Laplace transform is employed to approximately reduce the hypersingular boundary integral formulation given in the present paper into a system of linear algebraic equations. Once the linear algebraic equations are solved, the required physical solution is recovered through the use of a numerical method for inverting Laplace transform. To assess its validity and accuracy, the proposed numerical approach is applied to solve some specific problems.

2 Problem and model

An isotropic body is made up of two homogeneous materials that are possibly dissimilar. It has a geometry that does not vary along the z -direction. On the Oxy plane, the interface between the materials is the straight line segment Γ which lies on part of the x -axis between the points $(a, 0)$ and $(b, 0)$ (where a and b are given real numbers such that $a < b$). The exterior boundary of the body is a simple closed curve C comprising two parts, namely C^+ which lies above the x -axis and C^- below the axis. Figure 1 gives a geometrical sketch of the problem under consideration. Note that the regions enclosed by $C^+ \cup \Gamma$ and $C^- \cup \Gamma$ are denoted by R^+ and R^- respectively.

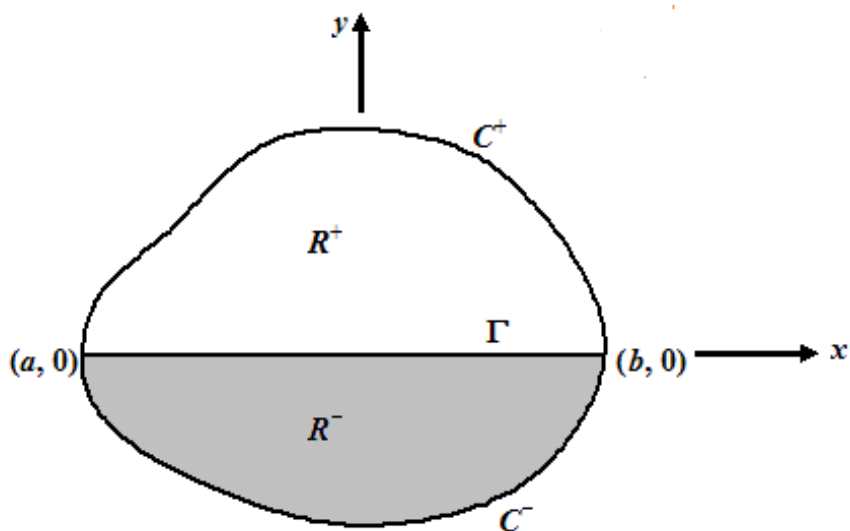


Figure 1: A geometrical sketch of the problem.

The body is deformed in such a way that the only non-zero component of the displacement is the one along the Oz direction, given by the function $w(x, y, t)$, where t denotes time. The non-vanishing components of the

Cartesian stress tensor are given by

$$\sigma_{xz} = \mu^\pm \frac{\partial w}{\partial x}, \quad \sigma_{yz} = \mu^\pm \frac{\partial w}{\partial y} \quad \text{for } (x, y) \in R^\pm, \quad (1)$$

where μ^+ and μ^- are the elastic shear moduli of the materials in R^+ and R^- respectively.

The interface Γ is microscopically damaged and exhibits viscoelastic behaviours. If the imperfect viscoelastic interface is macroscopically modelled using a distribution of linear springs and dashpots connected in parallel, as in Fan and Wang [8] (see also Ang and Fan [9]), then the following interfacial conditions hold:

$$\begin{aligned} \sigma_{yz}(x, 0^+, t) &= \sigma_{yz}(x, 0^-, t), \\ \sigma_{yz}(x, 0^+, t) &= \alpha \Delta w(x, t) + \beta \frac{\partial}{\partial t} [\Delta w(x, t)] \\ &\text{for } x \in (a, b) \text{ and } t > 0. \end{aligned} \quad (2)$$

where α and β are respectively the spring and the dashpot coefficients and $\Delta w(x, t) = w(x, 0^+, t) - w(x, 0^-, t)$ is the jump in the displacement across the imperfect interface. For homogeneous interface, α and β are constants.

The antiplane deformation of the materials in R^+ and R^- is governed by the two-dimensional wave equation

$$\frac{\partial^2 w}{\partial x^2} + \frac{\partial^2 w}{\partial y^2} = \frac{\rho^\pm}{\mu^\pm} \frac{\partial^2 w}{\partial t^2} \quad \text{for } (x, y) \in R^\pm \text{ and } t > 0, \quad (3)$$

where ρ^+ and ρ^- are the densities of the materials in R^+ and R^- respectively.

At each and every point on the exterior boundary $C = C^+ \cup C^-$, either the displacement w or the traction $p = \sigma_{xz}n_x + \sigma_{yz}n_y$ (but not both) is known. Note that $[n_x, n_y]$ is the unit normal vector to C , pointing away from the region R . In addition, since (3) contains a second order time derivative of w , it is necessary to specify w and $\partial w/\partial t$ throughout R^+ and R^- at time $t = 0$. Note that $\Delta w(x, 0)$ may be deduced from $w(x, y, 0)$.

The problem is to solve (3) for w subject to the known boundary data of either w or p at each point on C , the initial values of w and $\partial w/\partial t$ in $R^+ \cup R^-$ at $t = 0$ and the interfacial conditions in (2).

3 Integral formulation

Following closely the analysis in Ang and Fan [9], one may apply the reciprocal theorem for the two-dimensional Poisson's equation (in Clements [13]) to (3) to derive the integral equation (for $\eta \neq 0$)

$$\begin{aligned} \gamma(\xi, \eta)w(\xi, \eta, t) &= \iint_{R^+ \cup R^-} \Phi(x, y, \xi, \eta) \rho(x, y) \frac{\partial^2}{\partial t^2} w(x, y, t) dx dy \\ &+ \int_C [w(x, y, t) \mu(x, y) \frac{\partial}{\partial n} \Phi(x, y, \xi, \eta) \\ &- \Phi(x, y, \xi, \eta) p(x, y, t)] dS(x, y) \\ &- \int_a^b \Delta w(x, t) \mu^+ \frac{\partial}{\partial y} \Phi(x, y, \xi, \eta) \Big|_{y=0^+} dx, \end{aligned} \quad (4)$$

where $\gamma(\xi, \eta) = 1$ if (ξ, η) lies inside R^+ or R^- , $0 < \gamma(\xi, \eta) < 1$ if (ξ, η) lies on C^+ or C^- [$\gamma(\xi, \eta) = 1/2$ if (ξ, η) lies on a smooth part of C^+ or C^-], $\mu(x, y) = \mu^\pm$ if $(x, y) \in R^\pm$, $\rho(x, y) = \rho^\pm$ if $(x, y) \in R^\pm$ and $\Phi(x, y, \xi, \eta)$ is the Green's function for the corresponding perfect interface in an elastostatically deformed bimaterial as given by (Berger and Karageorghis [2])

$$\Phi(x, y, \xi, \eta) = \frac{1}{2\pi\mu^\pm} \operatorname{Re}\{\ln([x - \xi] + i[y - \eta])\} + \Phi^\pm(x, y, \xi, \eta) \quad \text{for } \pm y > 0, \quad (5)$$

$$\frac{\partial}{\partial n} \Phi(x, y, \xi, \eta) = n_x(x, y) \frac{\partial}{\partial x} \Phi(x, y, \xi, \eta) + n_y(x, y) \frac{\partial}{\partial y} \Phi(x, y, \xi, \eta), \quad (6)$$

$$\begin{aligned}\Phi^+(x, y, \xi, \eta) = & -\frac{\mu^- - \mu^+}{2\pi\mu^+(\mu^- + \mu^+)} \operatorname{Re}\{H(-\eta) \ln([x - \xi] + i[y - \eta]) \\ & + H(\eta) \ln([x - \xi] + i[y + \eta])\},\end{aligned}\quad (7)$$

$$\begin{aligned}\Phi^-(x, y, \xi, \eta) = & \frac{\mu^- - \mu^+}{2\pi\mu^-(\mu^- + \mu^+)} \operatorname{Re}\{H(-\eta) \ln([x - \xi] + i[-y - \eta]) \\ & + H(\eta) \ln([x - \xi] - i[y - \eta])\},\end{aligned}\quad (8)$$

with $i = \sqrt{-1}$ and H denoting the unit-step Heaviside function.

The function $\Phi(x, y, \xi, \eta)$ as given by (5), (7) and (8) is a modified fundamental solution of the two-dimensional Laplace's equation (for elastostatic problems) and it satisfies the conditions on the corresponding perfect interface. With $\Phi(x, y, \xi, \eta)$ thus given, the continuity of σ_{yz} on Γ as expressed on the first line of (2) is automatically satisfied by (4). It follows that the right hand side of the formulation (4) contains only one unknown function on the interface Γ , that is, the jump in the antiplane displacement w as denoted by $\Delta w(x, t)$.

Use of (1) and (4) gives

$$\begin{aligned}\sigma_{yz}(\xi, \eta, t) = & \mu^+ \iint_{R^+ \cup R^-} \frac{\partial}{\partial \eta} \Phi(x, y, \xi, \eta) \rho(x, y) \frac{\partial^2}{\partial t^2} w(x, y, t) dx dy \\ & + \mu^+ \int_C [w(x, y, t) \mu(x, y) \frac{\partial^2}{\partial n \partial \eta} \Phi(x, y, \xi, \eta) \\ & - p(x, y, t) \frac{\partial}{\partial \eta} \Phi(x, y, \xi, \eta)] dS(x, y) \\ & - (\mu^+)^2 \int_a^b \Delta w(x, t) \frac{\partial^2}{\partial y \partial \eta} \Phi(x, y, \xi, \eta) \Big|_{y=0^+} dx \\ & \text{for } (\xi, \eta) \text{ in the interior of } R^+.\end{aligned}\quad (9)$$

With (9), one may rewrite (2) as

$$\begin{aligned}
& \alpha \Delta w(\xi, t) + \beta \frac{\partial}{\partial t} \Delta w(\xi, t) \\
= & \mu^+ \lim_{\epsilon \rightarrow 0} \left\{ \iint_{R^+ \cup R^-} \frac{\partial}{\partial \eta} \Phi(x, y, \xi, \eta) \Big|_{\eta=|\epsilon|} \rho(x, y) \frac{\partial^2}{\partial t^2} w(x, y, t) dx dy \right. \\
& + \mu^+ \int_C [w(x, y, t) \mu(x, y) \left[\frac{\partial^2}{\partial n \partial \eta} \Phi(x, y, \xi, \eta) \right] \Big|_{\eta=|\epsilon|} \\
& \left. - p(x, y, t) \left[\frac{\partial}{\partial \eta} \Phi(x, y, \xi, \eta) \right] \Big|_{\eta=|\epsilon|}] dS(x, y) \right\} \\
& + \frac{\mu^+ \mu^-}{\pi(\mu^+ + \mu^-)} \mathcal{H} \int_a^b \frac{\Delta w(x, t)}{(\xi - x)^2} dx \\
& \text{for } a < \xi < b, \tag{10}
\end{aligned}$$

where \mathcal{H} denotes the integral over the interval $[a, b]$ is to be interpreted in the Hadamard finite-part sense as in Chen and Hong [14] or as given equivalently by the alternative definition (Ang and Clements [15])

$$\mathcal{H} \int_a^b \frac{F(x) dx}{(x - \xi)^2} \stackrel{\text{def}}{=} \lim_{\sigma \rightarrow 0^+} \left[\int_a^b \frac{(x - \xi)^2 F(x) dx}{[(x - \xi)^2 + \sigma^2]^2} - \frac{\pi}{2\sigma} F(\xi) \right] \text{ for } a < \xi < b. \tag{11}$$

Note that, because of the acceleration term in the governing partial differential equation, domain integrals over the region $R^+ \cup R^-$ appear in (4) and (10). In Section 4, the dual-reciprocity method that does not require the region R^+ and R^- to be discretised into finite elements or cells is applied to treat these integrals. A Laplace transform dual-reciprocity boundary element method based on (4) and (10) is then derived for the numerical solution of the problem described in Section 2. If one avoids collocating (4) at points on the interface but uses (10) instead to deal with the interfacial conditions (2) then the numerical procedure involves only one unknown function $\Delta w(x, t)$

on the interface. The Laplace transform is applied to remove the time derivatives in (4) and (10) and the final solution is recovered through the use of a numerical technique for inverting Laplace transform.

4 Numerical procedure

To develop a dual-reciprocity hypersingular boundary integral method for the problem in Section 2, the curves C^+ and C^- are discretised into N^+ and N^- straight line elements respectively. The elements from C^+ are denoted by $C_1^+, C_2^+, \dots, C_{N^+-1}^+$ and $C_{N^+}^+$ and those from C^- by $C_1^-, C_2^-, \dots, C_{N^--1}^-$ and $C_{N^-}^-$.

For collocation purpose, let the midpoint of the element C_k^\pm ($k = 1, 2, \dots, N^\pm$) be (ξ_k^\pm, η_k^\pm) . In addition, M^+ and M^- well-spaced out collocation points in the interior of R^+ and R^- respectively are chosen. The M^\pm interior points in R^\pm are denoted by (ξ_m^\pm, η_m^\pm) for $m = N^\pm + 1, N^\pm + 2, \dots, N^\pm + M^\pm$.

The dual-reciprocity method is applied to treat the domain integral in (4). To do this, the partial derivative $\partial^2 w / \partial t^2$ is approximated as

$$\begin{aligned} & \frac{\partial^2}{\partial t^2} w(x, y, t) \\ \simeq & \sum_{k=1}^{N^\pm+M^\pm} \frac{d^2}{dt^2} [w_k^\pm(t)] \sum_{j=1}^{N^\pm+M^\pm} \chi_{kj}^\pm \tau_j^\pm(x, y) \text{ for } (x, y) \in R^\pm, \end{aligned} \quad (12)$$

where $w_k^\pm(t) = w(\xi_k^\pm, \eta_k^\pm, t)$, the local interpolating functions $\tau_j^\pm(x, y)$ are given by

$$\tau_j^\pm(x, y) = 1 + ([x - \xi_j^\pm]^2 + [y - \eta_j^\pm]^2) + ([x - \xi_j^\pm]^2 + [y - \eta_j^\pm]^2)^{3/2}, \quad (13)$$

and the coefficients χ_{kj}^\pm are defined by

$$\sum_{k=1}^{N^\pm+M^\pm} \tau_j^\pm(\xi_k^\pm, \eta_k^\pm) \chi_{kp}^\pm = \delta_{jp}, \quad (14)$$

where δ_{jp} is the Kronecker-delta.

Note that the local interpolating functions in (13) are those proposed by Zhang and Zhu [16] and the coefficients χ_{kp}^\pm are the elements of the inverse of the $(N^\pm + M^\pm) \times (N^\pm + M^\pm)$ matrix $[\beta_{jk}^\pm]$, where $\beta_{jk}^\pm = \tau_j^\pm(\xi_k^\pm, \eta_k^\pm)$.

With (12), the domain integral in (4) can now be approximated as

$$\begin{aligned} & \iint_{R^+ \cup R^-} \Phi(x, y, \xi, \eta) \rho(x, y) \frac{\partial^2}{\partial t^2} w(x, y, t) dx dy \\ & \simeq \sum_{k=1}^{N^+ + M^+} \frac{\rho^+}{\mu^+} \Psi_k^+(\xi, \eta) \frac{d^2}{dt^2} [w_k^+(t)] \\ & \quad + \sum_{k=1}^{N^- + M^-} \frac{\rho^-}{\mu^-} \Psi_k^-(\xi, \eta) \frac{d^2}{dt^2} [w_k^-(t)], \end{aligned} \quad (15)$$

where

$$\begin{aligned} \Psi_k^\pm(\xi, \eta) &= \sum_{j=1}^{N^\pm + M^\pm} \chi_{kj}^\pm [\gamma^\pm(\xi, \eta) \theta_j^\pm(\xi, \eta) \\ & \quad + \int_{C^\pm \cup \Gamma} \mu^\pm [\Phi(x, y, \xi, \eta) \frac{\partial}{\partial n} \theta_j^\pm(x, y) \\ & \quad - \theta_j^\pm(x, y) \frac{\partial}{\partial n} \Phi(x, y, \xi, \eta)] dS(x, y)], \\ \gamma^+(\xi, \eta) &= \begin{cases} 1 & \text{if } (\xi, \eta) \in R^+ \\ 1/2 & \text{if } (\xi, \eta) \in C^+ \text{ (on smooth part)} \\ 0 & \text{if } (\xi, \eta) \in R^- \cup C^- \end{cases} \\ \gamma^-(\xi, \eta) &= \begin{cases} 1 & \text{if } (\xi, \eta) \in R^- \\ 1/2 & \text{if } (\xi, \eta) \in C^- \text{ (on smooth part)} \\ 0 & \text{if } (\xi, \eta) \in R^+ \cup C^+ \end{cases} \end{aligned}$$

$$\begin{aligned} \theta_j^\pm(x, y) &= \frac{1}{4} ([x - \xi_j^\pm]^2 + [y - \eta_j^\pm]^2) + \frac{1}{16} ([x - \xi_j^\pm]^2 + [y - \eta_j^\pm]^2)^2 \\ & \quad + \frac{1}{25} ([x - \xi_j^\pm]^2 + [y - \eta_j^\pm]^2)^{5/2}. \end{aligned} \quad (16)$$

Note that $C^\pm \cup \Gamma$ denotes the closed curve enclosing R^\pm and the unit normal vector $[n_x, n_y]$ on $C^\pm \cup \Gamma$ points out of R^\pm .

To treat the domain integral in (10), one may use (15) to derive

$$\begin{aligned} & \lim_{\epsilon \rightarrow 0} \iint_{R^+ \cup R^-} \frac{\partial}{\partial \eta} \Phi(x, y, \xi, \eta) \Big|_{\eta=|\epsilon|} \rho(x, y) \frac{\partial^2}{\partial t^2} w(x, y, t) dx dy \\ & \simeq \sum_{k=1}^{N^+ + M^+} \frac{\rho^+}{\mu^+} \Omega_k^+(\xi) \frac{d^2}{dt^2} [w_k^+(t)] + \sum_{k=1}^{N^- + M^-} \frac{\rho^-}{\mu^-} \Omega_k^-(\xi) \frac{d^2}{dt^2} [w_k^-(t)] \end{aligned} \quad (17)$$

for $a < \xi < b$,

where

$$\begin{aligned} \Omega_k^\pm(\xi) &= \sum_{j=1}^{N^\pm + M^\pm} \chi_{kj}^\pm \left[-\kappa \frac{\partial}{\partial \eta} \theta_j^\pm(\xi, \eta) \Big|_{\eta=0} \right. \\ &+ \lim_{\epsilon \rightarrow 0} \int_{C^\pm} \mu^\pm \frac{\partial}{\partial \eta} [\Phi(x, y, \xi, \eta)] \Big|_{\eta=|\epsilon|} \frac{\partial}{\partial n} \theta_j^\pm(x, y) dS(x, y) \\ &- \lim_{\epsilon \rightarrow 0} \int_{C^\pm} \mu^\pm \theta_j^\pm(x, y) \frac{\partial^2}{\partial \eta \partial n} \Phi(x, y, \xi, \eta) \Big|_{\eta=|\epsilon|} dS(x, y) \\ &\left. \pm \frac{\kappa}{\pi} \mathcal{H} \int_a^b \frac{\theta_j^\pm(x, 0)}{(x - \xi)^2} dx \right], \end{aligned} \quad (18)$$

where $\kappa = -\mu^- / (\mu^+ + \mu^-)$.

Over the boundary element C_m^\pm ($m = 1, 2, \dots, N^\pm$), the antiplane displacement w and traction p are assumed to be spatially invariant given respectively by $w_m^\pm(t)$ and $p_m^\pm(t)$, where $w_m^\pm(t) = w(\xi_m^\pm, \eta_m^\pm, t)$ and $p_m^\pm(t) = p(\xi_m^\pm, \eta_m^\pm, t)$. For the approximation of the antiplane displacement jump across the interface, that is, $\Delta w(x, t)$, the interface Γ given by the interval $[a, b]$ (on the x -axis) is divided into P subintervals (elements) $[x_0, x_1]$, $[x_1, x_2]$, \dots , $[x_{P-2}, x_{P-1}]$ and $[x_{P-1}, x_P]$, where $x_0 = a$, $x_P = b$ and $x_j < x_{j+1}$ for $j = 1, 2, \dots, P - 1$. The displacement jump $\Delta w(x, t)$ is approximated by a spatially invariant function $\Delta w_j(t)$ over the subinterval $[x_{j-1}, x_j]$.

Letting $(\xi, \eta) = (\xi_m^\pm, \eta_m^\pm)$ ($m = 1, 2, \dots, N^\pm + M^\pm$) in (4) and using (15), one may then approximately obtain

$$\begin{aligned}
& \gamma(\xi_m^+, \eta_m^+) w_m^+(t) \\
&= \sum_{k=1}^{N^+ + M^+} \frac{\rho^+}{\mu^+} \Psi_k^+(\xi_m^+, \eta_m^+) \frac{d^2}{dt^2} [w_k^+(t)] + \sum_{k=1}^{N^- + M^-} \frac{\rho^-}{\mu^-} \Psi_k^-(\xi_m^+, \eta_m^+) \frac{d^2}{dt^2} [w_k^-(t)] \\
&+ \sum_{k=1}^{N^+} \int_{C_k^+} [\mu^+ w_k^+(t) \frac{\partial}{\partial n} \Phi(x, y, \xi_m^+, \eta_m^+) - p_k^+(t) \Phi(x, y, \xi_m^+, \eta_m^+)] dS(x, y) \\
&+ \sum_{k=1}^{N^-} \int_{C_k^-} [\mu^- w_k^-(t) \frac{\partial}{\partial n} \Phi(x, y, \xi_m^+, \eta_m^+) - p_k^-(t) \Phi(x, y, \xi_m^+, \eta_m^+)] dS(x, y) \\
&- \sum_{j=1}^P \Delta w_j(t) \int_{x_{j-1}}^{x_j} \mu^+ \frac{\partial}{\partial y} \Phi(x, y, \xi_m^+, \eta_m^+) \Big|_{y=0^+} dx \\
&\quad \text{for } m = 1, 2, \dots, N^+ + M^+, \tag{19}
\end{aligned}$$

and

$$\begin{aligned}
& \gamma(\xi_m^-, \eta_m^-) w_m^-(t) \\
&= \sum_{k=1}^{N^+ + M^+} \frac{\rho^+}{\mu^+} \Psi_k^+(\xi_m^-, \eta_m^-) \frac{d^2}{dt^2} [w_k^+(t)] + \sum_{k=1}^{N^- + M^-} \frac{\rho^-}{\mu^-} \Psi_k^-(\xi_m^-, \eta_m^-) \frac{d^2}{dt^2} [w_k^-(t)] \\
&+ \sum_{k=1}^{N^+} \int_{C_k^+} [\mu^+ w_k^+(t) \frac{\partial}{\partial n} \Phi(x, y, \xi_m^-, \eta_m^-) - p_k^+(t) \Phi(x, y, \xi_m^-, \eta_m^-)] dS(x, y) \\
&+ \sum_{k=1}^{N^-} \int_{C_k^-} [\mu^- w_k^-(t) \frac{\partial}{\partial n} \Phi(x, y, \xi_m^-, \eta_m^-) - p_k^-(t) \Phi(x, y, \xi_m^-, \eta_m^-)] dS(x, y) \\
&- \sum_{j=1}^P \Delta w_j(t) \int_{x_{j-1}}^{x_j} \mu^+ \frac{\partial}{\partial y} \Phi(x, y, \xi_m^-, \eta_m^-) \Big|_{y=0^+} dx \\
&\quad \text{for } m = 1, 2, \dots, N^- + M^-. \tag{20}
\end{aligned}$$

Note that either $w_k^\pm(t)$ or $p_k^\pm(t)$ (not both) is known over the element C_k^\pm . Thus, there are $N^+ + M^+ + N^- + M^- + P$ unknown functions of t as given by either $w_k^\pm(t)$ or $p_k^\pm(t)$ for $k = 1, 2, \dots, N^\pm$, $w_m^\pm(t)$ for $m = N^\pm + 1, N^\pm + 2, \dots, N^\pm + M^\pm$, and $\Delta w_j(t)$ for $j = 1, 2, \dots, P$. To complete the system, another P equations are set up by letting $\xi = q_m$ ($m = 1, 2, \dots, P$) in (10), where $q_m = (x_{m-1} + x_m)/2$, to obtain

$$\begin{aligned}
& \alpha \Delta w_m(t) + \beta \frac{d}{dt} \Delta w_m(t) \\
= & \sum_{k=1}^{N^+ + M^+} \rho^+ \Omega_k^+(q_m) \frac{d^2}{dt^2} [w_k^+(t)] + \sum_{k=1}^{N^- + M^-} \frac{\mu^+ \rho^-}{\mu^-} \Omega_k^-(q_m) \frac{d^2}{dt^2} [w_k^-(t)] \\
& + \mu^+ \sum_{k=1}^{N^+} \int_{C_k^+} [w_k^+(t) \mu^+ \left[\frac{\partial^2}{\partial n \partial \eta} \Phi(x, y, q_m, \eta) \right] \Big|_{\eta=0^+} \\
& - p_k^+(t) \left[\frac{\partial}{\partial \eta} \Phi(x, y, q_m, \eta) \right] \Big|_{\eta=0^+}] dS(x, y) \\
& + \mu^+ \sum_{k=1}^{N^-} \int_{C_k^-} [w_k^-(t) \mu^- \left[\frac{\partial^2}{\partial n \partial \eta} \Phi(x, y, q_m, \eta) \right] \Big|_{\eta=0^+} \\
& - p_k^-(t) \left[\frac{\partial}{\partial \eta} \Phi(x, y, q_m, \eta) \right] \Big|_{\eta=0^+}] dS(x, y) \\
& + \frac{\mu^+ \mu^-}{\pi(\mu^+ + \mu^-)} \sum_{j=1}^P \Delta w_j(t) \left[\frac{1}{q_m - x_j} - \frac{1}{q_m - x_{j-1}} \right] \\
& \qquad \qquad \qquad \text{for } m = 1, 2, \dots, P. \tag{21}
\end{aligned}$$

Let us denote the Laplace transform of a function $f(t)$ by $\widehat{f}(s)$, that is,

$$\widehat{f}(s) = \int_0^\infty f(t) \exp(-st) dt, \tag{22}$$

where s is the Laplace transform parameter.

In the Laplace transform domain, (19), (20) and (21) are respectively

given by

$$\begin{aligned}
\gamma(\xi_m^+, \eta_m^+) \widehat{w}_m^+(s) &= \sum_{k=1}^{N^++M^+} \frac{\rho^+}{\mu^+} \Psi_k^+(\xi_m^+, \eta_m^+) [s^2 \widehat{w}_k^+(s) - s w_k^+(0) - \left. \frac{d}{dt} [w_k^+(t)] \right|_{t=0}] \\
&+ \sum_{k=1}^{N^-+M^-} \frac{\rho^-}{\mu^-} \Psi_k^-(\xi_m^+, \eta_m^+) [s^2 \widehat{w}_k^-(s) - s w_k^-(0) - \left. \frac{d}{dt} [w_k^-(t)] \right|_{t=0}] \\
&+ \sum_{k=1}^{N^+} \int_{C_k^+} [\mu^+ \widehat{w}_k^+(s) \frac{\partial}{\partial n} \Phi(x, y, \xi_m^+, \eta_m^+) - \widehat{p}_k^+(s) \Phi(x, y, \xi_m^+, \eta_m^+)] dS(x, y) \\
&+ \sum_{k=1}^{N^-} \int_{C_k^-} [\mu^- \widehat{w}_k^-(s) \frac{\partial}{\partial n} \Phi(x, y, \xi_m^+, \eta_m^+) - \widehat{p}_k^-(s) \Phi(x, y, \xi_m^+, \eta_m^+)] dS(x, y) \\
&- \sum_{j=1}^P \Delta \widehat{w}_j(s) \int_{x_{j-1}}^{x_j} \mu^+ \frac{\partial}{\partial y} \Phi(x, y, \xi_m^+, \eta_m^+) \Big|_{y=0^+} dx \\
&\text{for } m = 1, 2, \dots, N^+ + M^+, \tag{23}
\end{aligned}$$

$$\begin{aligned}
\gamma(\xi_m^-, \eta_m^-) \widehat{w}_m^-(s) &= \sum_{k=1}^{N^++M^+} \frac{\rho^+}{\mu^+} \Psi_k^+(\xi_m^-, \eta_m^-) [s^2 \widehat{w}_k^+(s) - s w_k^+(0) - \left. \frac{d}{dt} [w_k^+(t)] \right|_{t=0}] \\
&+ \sum_{k=1}^{N^-+M^-} \frac{\rho^-}{\mu^-} \Psi_k^-(\xi_m^-, \eta_m^-) [s^2 \widehat{w}_k^-(s) - s w_k^-(0) - \left. \frac{d}{dt} [w_k^-(t)] \right|_{t=0}] \\
&+ \sum_{k=1}^{N^+} \int_{C_k^+} [\mu^+ \widehat{w}_k^+(s) \frac{\partial}{\partial n} \Phi(x, y, \xi_m^-, \eta_m^-) - \widehat{p}_k^+(s) \Phi(x, y, \xi_m^-, \eta_m^-)] dS(x, y) \\
&+ \sum_{k=1}^{N^-} \int_{C_k^-} [\mu^- \widehat{w}_k^-(s) \frac{\partial}{\partial n} \Phi(x, y, \xi_m^-, \eta_m^-) - \widehat{p}_k^-(s) \Phi(x, y, \xi_m^-, \eta_m^-)] dS(x, y) \\
&- \sum_{j=1}^P \Delta \widehat{w}_j(s) \int_{x_{j-1}}^{x_j} \mu^+ \frac{\partial}{\partial y} \Phi(x, y, \xi_m^-, \eta_m^-) \Big|_{y=0^+} dx \\
&\text{for } m = 1, 2, \dots, N^- + M^-, \tag{24}
\end{aligned}$$

and

$$\begin{aligned}
& \alpha \Delta \widehat{w}_m(s) + \beta [s \Delta \widehat{w}_m(s) - \Delta w_m(0)] \\
= & \sum_{k=1}^{N^+ + M^+} \rho^+ \Omega_k^+(q_m) [s^2 \widehat{w}_k^+(s) - s w_k^+(0) - \left. \frac{d}{dt} [w_k^+(t)] \right|_{t=0}] \\
& + \sum_{k=1}^{N^- + M^-} \frac{\mu^+ \rho^-}{\mu^-} \Omega_k^-(q_m) [s^2 \widehat{w}_k^-(s) - s w_k^-(0) - \left. \frac{d}{dt} [w_k^-(t)] \right|_{t=0}] \\
& + \mu^+ \sum_{k=1}^{N^+} \int_{C_k^+} [\widehat{w}_k^+(s) \mu^+ \left[\frac{\partial^2}{\partial n \partial \eta} \Phi(x, y, q_m, \eta) \right] \Big|_{\eta=0^+} \\
& - \widehat{p}_k^+(s) \left[\frac{\partial}{\partial \eta} \Phi(x, y, q_m, \eta) \right] \Big|_{\eta=0^+}] dS(x, y) \\
& + \mu^+ \sum_{k=1}^{N^-} \int_{C_k^-} [\widehat{w}_k^-(s) \mu^- \left[\frac{\partial^2}{\partial n \partial \eta} \Phi(x, y, q_m, \eta) \right] \Big|_{\eta=0^+} \\
& - \widehat{p}_k^-(s) \left[\frac{\partial}{\partial \eta} \Phi(x, y, q_m, \eta) \right] \Big|_{\eta=0^+}] dS(x, y) \\
& + \frac{\mu^+ \mu^-}{\pi(\mu^+ + \mu^-)} \sum_{j=1}^P \Delta \widehat{w}_j(s) \left[\frac{1}{q_m - x_j} - \frac{1}{q_m - x_{j-1}} \right] \\
& \qquad \qquad \qquad \text{for } m = 1, 2, \dots, P. \quad (25)
\end{aligned}$$

Note that $\widehat{w}_k^\pm(s)$, $\widehat{p}_k^\pm(s)$ and $\Delta \widehat{w}_m(s)$ are the Laplace transform of $w_k^\pm(t)$, $p_k^\pm(t)$ and $\Delta w_m(t)$ respectively.

From the initial conditions of the problem under consideration, $w_k^\pm(t)$, $d[w_k^\pm(t)]/dt$ and $\Delta w_m(t)$ are known at $t = 0$. On C_k^+ , either $\widehat{w}_k^+(s)$ or $\widehat{p}_k^+(s)$ (not both) is known from the Laplace transform of the prescribed boundary conditions. Similarly, on C_k^- , either $\widehat{w}_k^-(s)$ or $\widehat{p}_k^-(s)$ is prescribed. Thus, (23), (24) and (25) constitute a system of $N^+ + M^+ + N^- + M^- + P$ linear algebraic equations containing $N^+ + M^+ + N^- + M^- + P$ unknown functions of s . Once these unknowns are determined for selected values of s , a numer-

ical technique (as explained below) may be applied to recover the required physical solution.

5 Numerical inversion of Laplace transform

The Stehfest's method for the numerical inversion of Laplace transform has been applied successfully to solve quite a wide range of engineering problems (see, for example, Moench and Ogata [17], Ang [1], Zhu *et al.* [18] and Sladek *et al.* [19]). According to Stehfest [20], if $\hat{f}(s)$ in (22) is known, $f(t)$ is approximately given by

$$f(t) \simeq \frac{\ln(2)}{t} \sum_{n=1}^L v_n \hat{f}\left(\frac{n \ln(2)}{t}\right), \quad (26)$$

where L is an even integer and

$$v_n = (-1)^{n+L/2} \sum_{m=\lceil (n+1)/2 \rceil}^{\min(n, L/2)} \frac{m^{L/2} (2m)!}{(L/2 - m)! m! (m-1)! (n-m)! (2m-n)!} \quad (27)$$

with $[r]$ being the integer part of the real number r .

Most (if not all) numerical techniques for inverting Laplace transform are highly susceptible to errors in the calculation of $\hat{f}(s)$. Formula (26) is no exception. Theoretically, the integer L which denotes the number of terms in (26) should be selected to be as large as possible. However, in practice, due to the limitation of computers as finite machines which store real numbers in truncated form and possible numerical errors in $\hat{f}(s)$, the approximation (26) may start to deteriorate rapidly once L exceeds a critical value. The coefficient v_n increases in magnitude with increasing n . Thus, the sum in (26) may contain extremely large magnitude terms which do not cancel each other properly due to errors if L is too large. The critical value of L depends on the arithmetical precision of the calculation as well as the accuracy in the

evaluation of $\widehat{f}(s)$ (Stehfest [20]). If a higher arithmetical precision is used or if $\widehat{f}(s)$ is computed more accurately, the critical value is larger.

Perhaps a possible method for finding suitable values of L for any problem is through testing the computer code developed for special cases with known solutions. To obtain a rough idea of the range of the value L that may be used to invert Laplace transform dual-reciprocity boundary element solutions of dynamic problems in engineering, one may refer to relevant works in the literature. For example, Zhu *et al.* [18] reported that their numerical results for particular test problems solved using double precision arithmetics and constant elements did not change significantly when the value of L was increased from 6 to 16. Sladek *et al.* [19] obtained a Laplace transform solution of a dynamic crack problem using a meshless local boundary integral equation method and used $L = 10$ to invert the Laplace transform.

6 Specific problems

Problem 1. For a specific test problem, we take

$$\mu^+ = 1/5, \mu^- = 1/2, \rho^+ = 1/5 \text{ and } \rho^- = 1/2, \quad (28)$$

and the regions R^+ and R^- to be

$$\begin{aligned} R^+ &= \{(x, y) : 0 < x < 1, 0 < y < 1/2\}, \\ R^- &= \{(x, y) : 0 < x < 1, -1/2 < y < 0\}. \end{aligned} \quad (29)$$

Furthermore, we require the unknown stress $\sigma_{yz}(x, y, t)$ and the displacement jump $\Delta w(x, t)$ to satisfy the interfacial conditions

$$\begin{aligned} \sigma_{yz}(x, 0^+, t) &= \sigma_{yz}(x, 0^-, t) \\ &= \frac{\sqrt{26}}{40} \Delta w(x, t) + \frac{\sqrt{26}}{40} \frac{\partial}{\partial t} [\Delta w(x, t)] \\ &\text{for } x \in (0, 1) \text{ and } t > 0. \end{aligned} \quad (30)$$

A solution of (3) satisfying (30) [with μ^+ , μ^- , ρ^+ and ρ^- as given by (28)] is

$$\begin{aligned}
w(x, y, t) = & H(y) \left\{ \left[\frac{1}{10} \cosh\left(\frac{\sqrt{26}}{5}y\right) + \frac{1}{10} \sinh\left(\frac{\sqrt{26}}{5}y\right) \right] \cos(x) \exp\left(-\frac{t}{5}\right) \right\} \\
& + H(-y) \left\{ \left[-\frac{1}{10} \cosh\left(\frac{\sqrt{26}}{5}y\right) + \frac{1}{25} \sinh\left(\frac{\sqrt{26}}{5}y\right) \right] \right. \\
& \left. \times \cos(x) \exp\left(-\frac{t}{5}\right) \right\} + \sin\left(\frac{t}{5}\right) \cos\left(\frac{y}{5}\right). \tag{31}
\end{aligned}$$

To devise a test problem, we use (31) to generate boundary values of the displacement w on the sides $y = \pm 1/2$, $0 < x < 1$, boundary values of the traction p on $x = 0$, $-1/2 < y < 1/2$ and also on $x = 1$, $-1/2 < y < 1/2$ and initial values of w and $\partial w / \partial t$ at $t = 0$ in R^+ and R^- . The numerical procedure outlined above is then applied to solve (3) subject to the initial-boundary data thus generated and the interfacial conditions (30). If the procedure really works, we should recover approximately the solution (31) and the displacement jump $\Delta w(x, t)$ approximately at selected time instants. From (31), the exact $\Delta w(x, t)$ is given by

$$\Delta w(x, t) = \frac{1}{5} \cos(x) \exp\left(-\frac{t}{5}\right). \tag{32}$$

Each side of the square region $0 < x < 1$, $-1/2 < y < 1/2$, is divided into J boundary elements of equal length. To avoid ambiguity, J is chosen to be even so that a boundary element is entirely in either R^+ or R^- (though one of the endpoints of an element may lie on Γ). Thus, $N^+ = N^- = 2J$. Furthermore, the $M^+ + M^-$ collocation points in the interior of R^+ and R^- are chosen to be given by $(i/(K_1 + 1), j/[2(K_2 + 1)])$ for $i = 1, 2, \dots, K_1$ and $j = \pm 1, \pm 2, \dots, \pm K_2$, where K_1 and K_2 are positive integers. Note that $M^+ = M^- = K_1 K_2$. Thus, there are $2K_1 K_2$ interior collocation points. For example, the 12 interior collocation points generated by $(K_1, K_2) = (3, 2)$ are as shown in Figure 2. The interface Γ is divided into P elements of equal length.

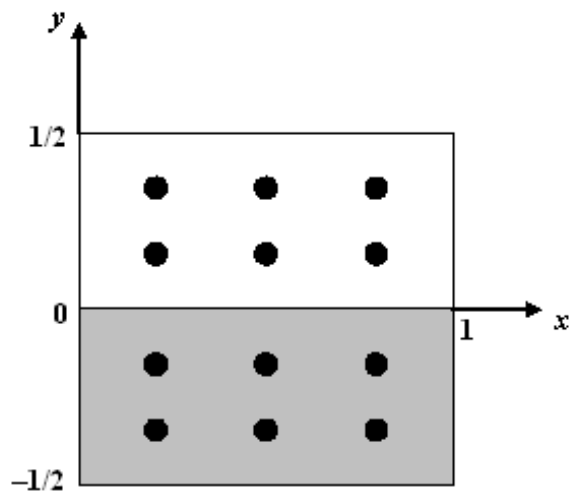


Figure 2: Distribution of the interior collocation points generated using $(K_1, K_2) = (3, 2)$.

Table 1. Numerical and exact values of the displacement w at selected interior points and time $t = 1$ are compared (Problem 1).

Point (x, y)	$J = P = 6$ $(K_1, K_2) = (3, 1)$ $L = 6$	$J = P = 18$ $(K_1, K_2) = (7, 3)$ $L = 10$	Exact
$(0.25, 0.25)$	0.29902	0.30129	0.30078
$(0.50, 0.25)$	0.28942	0.29116	0.29114
$(0.75, 0.25)$	0.27469	0.27631	0.27572
$(0.25, -0.25)$	0.10529	0.10815	0.10832
$(0.50, -0.25)$	0.11378	0.11668	0.11682
$(0.75, -0.25)$	0.12704	0.13018	0.13038

In Table 1, we compare the numerical values of w at various selected interior points at time $t = 1$ with the exact solution (31). The numerical

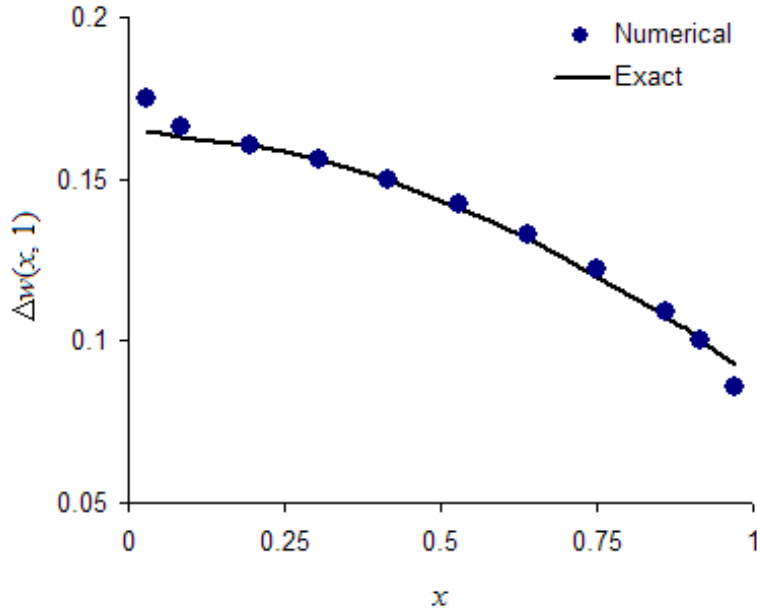


Figure 3: A graphical comparison between numerical and exact $\Delta w(x, 1)$ for $0 < x < 1$ (Problem 1).

values in the second column of the table are obtained using $J = P = 6$ (24 exterior boundary elements and 6 interfacial elements, each of length $1/6$ units), $(K_1, K_2) = (3, 1)$ (6 interior collocation points) and $L = 6$ [6 terms in the Stehfest's formula (26)]. When the test problem under consideration is solved more accurately in the Laplace transform domain by using more elements and interior collocation points, more terms may be employed in the Stehfest's formula. Thus, in the third column of Table 1, with $J = P = 18$ (72 exterior boundary elements and 18 interfacial elements, each of length $1/18$) and $(K_1, K_2) = (7, 3)$ (42 interior collocation points), the numerical values are obtained by using $L = 10$ in (26) to invert the numerical solution in the Laplace transform domain. It is obvious that the numerical values in the third column are more accurate compared with those in the second

column.

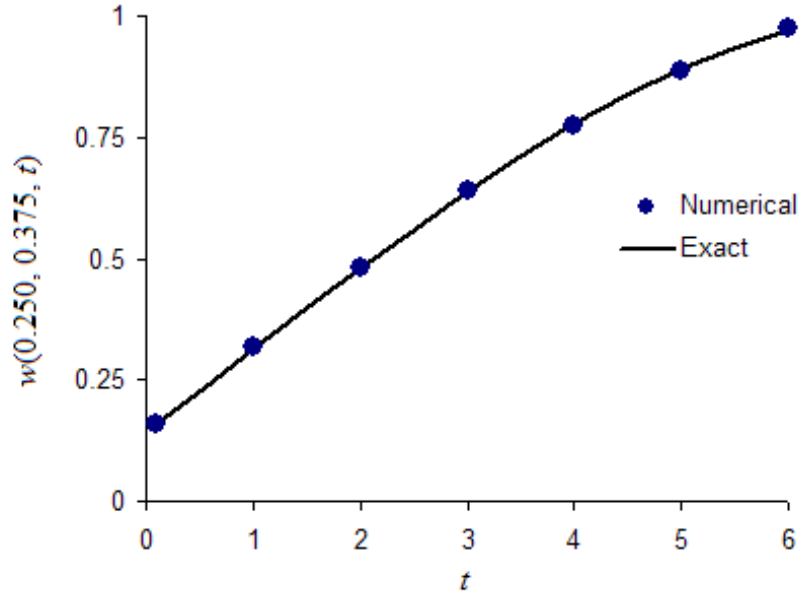


Figure 4: A graphical comparison between numerical and exact $w(0.250, 0.375, t)$ over the time interval $0 < t < 6$ (Problem 1).

In Figure 3, some numerical values of the interfacial displacement jump $\Delta w(x, t)$ obtained using $J = P = 18$, $(K_1, K_2) = (7, 3)$ and $L = 10$ are compared against the graph of (32) over the interval $0 < x < 1$ at time $t = 1$. There is a reasonably good agreement between the numerical and the exact interfacial displacement jump except at interfacial points which are very close to the exterior sides $x = 0$ and $x = 1$ of the bimaterial. However, it is possible to improve the accuracy of the numerical values at those points by refining the computation, such as by employing more interfacial elements near $x = 0$ and $x = 1$.

In Figure 4, some numerical values of $w(x, y, t)$ at $(0.250, 0.375)$, as ob-

tained using $J = P = 18$, $(K_1, K_2) = (7, 3)$ and $L = 10$, are compared against the graph of the exact solution (31) over the time interval $0 < t < 6$. The numerical values agree well with the exact solution over the time interval under consideration.

Problem 2. In Problem 1 above, note that $\rho^+/\mu^+ = \rho^-/\mu^-$, that is, the waves travel at the same speed in both regions R^+ and R^- . Furthermore, $\Delta w(x, t)$ differs from $\partial[\Delta w(x, t)]/\partial t$ by a mere constant factor and does not vary sinusoidally with time. For a test problem in which ρ^+/μ^+ is not equal to ρ^-/μ^- and $\Delta w(x, t)$ varies sinusoidally with time, choose

$$\mu^+ = 1, \mu^- = 2, \rho^+ = 1 \text{ and } \rho^- = 1/2, \quad (33)$$

and take the unknown stress $\sigma_{yz}(x, y, t)$ and the displacement jump $\Delta w(x, t)$ to satisfy the interfacial conditions

$$\begin{aligned} \sigma_{yz}(x, 0^+, t) &= \sigma_{yz}(x, 0^-, t) \\ &= \Delta w(x, t) + \frac{\partial}{\partial t}[\Delta w(x, t)] \\ &\text{for } x \in (0, 1) \text{ and } t > 0. \end{aligned} \quad (34)$$

It is easy to check that a solution of (3) satisfying (34) [with μ^+ , μ^- , ρ^+ and ρ^- as given by (33)] is given by

$$\begin{aligned} w(x, y, t) &= H(y)\left\{-\frac{1}{2}\cos(t) + \frac{1}{2}\sin(t)\right\}\cos(y) \\ &\quad + \sin(t)\sin(y) + \sin(2t)\sin(2y) \\ &\quad + H(-y)\left\{\frac{4}{5}\cos(2t) - \frac{2}{5}\sin(2t)\right\}\cos(y) \\ &\quad + \sin(t)\sin\left(\frac{y}{2}\right) + \sin(2t)\sin(y)\}. \end{aligned} \quad (35)$$

Note that the displacement jump $\Delta w(x, t)$ corresponding to (35) is

$$\Delta w(x, t) = -\frac{1}{2}\cos(t) + \frac{1}{2}\sin(t) - \frac{4}{5}\cos(2t) + \frac{2}{5}\sin(2t). \quad (36)$$

For the test problem, the regions R^+ and R^- are as defined in (29) and (35) is used to generate boundary values of the displacement w on all the four sides of the square bimaterial as well as initial values of w and $\partial w/\partial t$ at $t = 0$ in R^+ and R^- . The numerical procedure outlined above is then applied to solve (3) subject to the initial-boundary data thus generated and the interfacial conditions (34).

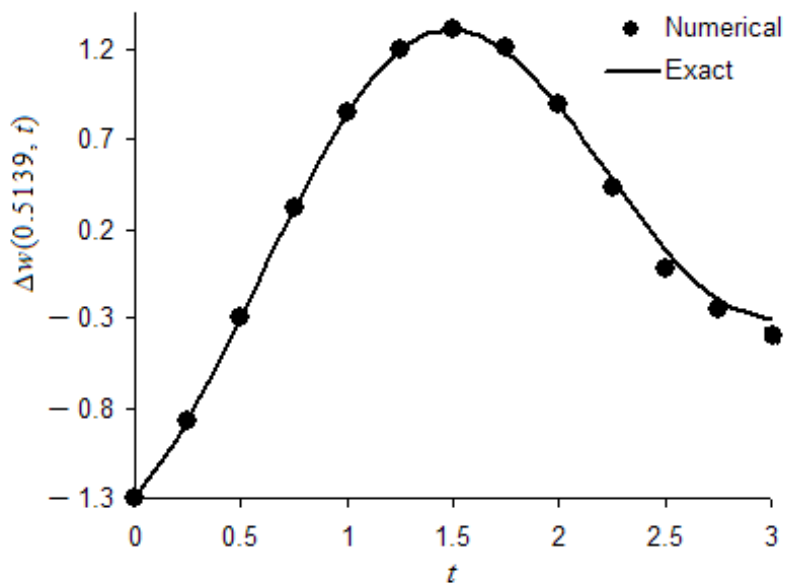


Figure 5: A graphical comparison between numerical and exact $\Delta w(0.5139, t)$ over the time interval $0 < t < 3$ (Problem 2).

The exterior boundary of the solution domain is discretised into $4J$ equal length elements and the $2K_1K_2$ interior collocation points are chosen as in Problem 1 above. In Figure 5, the numerical displacement jump $\Delta w(x, t)$, as obtained by using $J = P = 36$, $(K_1, K_2) = (8, 4)$ and $L = 18$, is compared graphically with the exact value given by (35) at the interfacial point

(0.5139, 0) over the time interval $0 < t < 3$.

Problem 3. For a particular problem with a physical interpretation, consider two dissimilar elastic slabs R^+ and R^- which occupy the regions $0 < x < \ell$, $0 < y < \ell/2$, and $0 < x < \ell$, $-\ell/2 < y < 0$, respectively, and are joined along the plane boundary $0 < x < \ell$, $y = 0$. Here ℓ is a given constant length. The elastic material in R^\pm is homogeneous with shear modulus μ^\pm and mass density ρ^\pm . The slab is subject to an antiplane elastodynamic deformation governed by (3) with the initial-boundary conditions

$$\begin{aligned} w(x, y, 0) &= 0 \text{ and } \left. \frac{\partial}{\partial t}[w(x, y, t)] \right|_{t=0} = 0 \text{ for } (x, y) \in R^+ \cup R^-, \\ w(x, -\frac{1}{2}\ell, t) &= 0 \text{ and } \sigma_{yz}(x, \frac{1}{2}\ell, t) = H(t)\sigma_0 \text{ for } 0 < x < \ell \text{ and } t > 0, \\ \sigma_{xz}(0, y, t) &= 0 \text{ and } \sigma_{xz}(\ell, y, t) = 0 \text{ for } -\frac{1}{2}\ell < y < \frac{1}{2}\ell \text{ and } t > 0, \end{aligned} \quad (37)$$

where σ_0 is a given constant. In addition, the interface between the slabs is viscoelastic such that (2) holds.

The exterior boundary of the bimaterial slab is discretised into $4J$ equal length elements and $2K_1K_2$ interior collocation points are chosen as in Problem 1 above (with $\ell = 1$). The numerical procedure in Section 4 is then applied using $J = P = 18$, $(K_1, K_2) = (7, 3)$ and $L = 10$ in order to compute the displacement field in the slab and the displacement jump across the imperfect viscoelastic interface. Taking $\mu^+/\mu^- = 5/4$, $\rho^+/\rho^- = 5/3$ and $\beta/\sqrt{\mu^+\rho^+} = 100$, we plot the non-dimensionalised interfacial displacement jump $\mu^+\Delta w(x, t)/(\sigma_0\ell)$ against the non-dimensionalised time variable $\sqrt{\mu^+}t/(\ell\sqrt{\rho^+})$ at $x/\ell = 0.5278$ for selected values of $\ell\alpha/\mu^+$ in Figure 6. Note that for this particular problem Δw is independent of x . Also, due to the discontinuity in the load function at $t = 0$, it may be difficult to obtain sensible numerical results for $\mu^+\Delta w(x, t)/(\sigma_0\ell)$ when the non-dimensionalised

time variable $\sqrt{\mu^+ t}/(\ell\sqrt{\rho^+})$ is extremely small. However, the computation of $\mu^+ \Delta w(x, t)/(\sigma_0 \ell)$ for the range of $\sqrt{\mu^+ t}/(\ell\sqrt{\rho^+})$ which is of practical interest presents no considerable difficulty. As may be expected, for each value of $\ell\alpha/\mu^+$ in Figure 6, the non-dimensionalised displacement jump $\mu^+ \Delta w(x, t)/(\sigma_0 \ell)$ rises rapidly to reach a local peak before settling down to the steady-state value of $\mu^+ /(\ell\alpha)$.

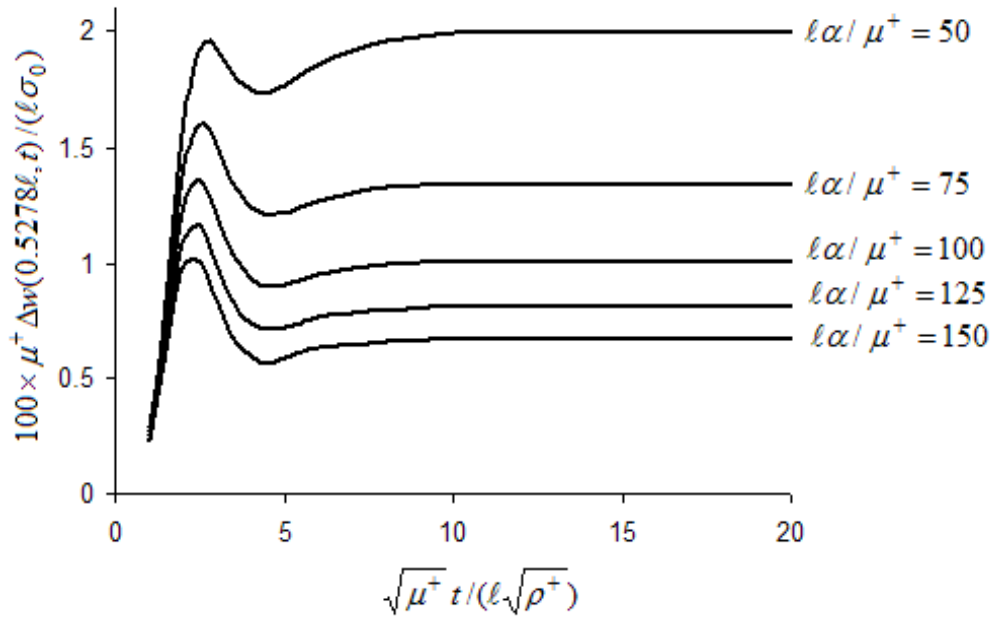


Figure 6: Plots of $\mu^+ \Delta w(x, t)/(\sigma_0 \ell)$ against the non-dimensionalised time variable $\sqrt{\mu^+ t}/(\ell\sqrt{\rho^+})$ at $x/\ell = 0.5278$ for selected values of $\ell\alpha/\mu^+$ (Problem 3).

7 Summary and discussion

A dual-reciprocity hypersingular boundary integral method is devised for solving numerically an antiplane elastodynamic problem involving a bima-

terial with an imperfect viscoelastic interface. The condition which models the imperfect viscoelastic interface as a distribution of linear springs and dashpots connected in parallel is expressed in terms of a hypersingular integral equation. In such a hypersingular boundary integral formulation, the interfacial displacement jump is the only unknown function on the interface.

In implementing the method, it is not necessary to discretise the region occupied by the bimaterial but only its exterior boundary and the interface. The method reduces the problem under consideration to a system of linear algebraic equations of the form $\mathbf{A}\mathbf{X} = \mathbf{B}$ (where \mathbf{A} is a known $N \times N$ matrix, \mathbf{X} is an $N \times 1$ matrix containing the unknown parameters in the formulation and \mathbf{B} is a given $N \times 1$ matrix) in the Laplace transform domain. The computation of the matrix \mathbf{A} takes up the main bulk of the computer time. Fortunately, the calculations involved are mostly independent of the Laplace transform parameter. Thus, although $\mathbf{A}\mathbf{X} = \mathbf{B}$ has to be solved for several different values of the Laplace transform parameter, the computationally intensive portion of the numerical procedure has to be carried out only once. After the heavy computation is completed, the system of linear algebraic equations may be set up and solved using a relatively small amount of computer time for different values of the Laplace transform parameter. Once \mathbf{X} is determined numerically for several selected values of the Laplace transform parameter, it may be inverted numerically by using the Stehfest's method to obtain the interfacial displacement jump as well as the displacements at selected points in the bimaterial.

The proposed method is applied to solve some specific problems. For the problems with known solutions, the numerical values of the displacement and the interfacial displacement jump show good agreement with the exact solution. Improved accuracy is also observed in the numerical values when the calculations are refined by using more boundary and interfacial elements

and more terms in the Stehfest's method. This suggests the method may be applied successfully to solve this class of elastodynamic problems involving an imperfect viscoelastic interface in a bimaterial.

The numerical procedure described in the present paper employs only constant boundary and interfacial elements. The accuracy of the solution in the Laplace transform domain may be improved through the use of higher order elements, such as the discontinuous linear elements (refer to, for example, París and Cañas [22] and Ang [21]), instead of increasing the number of constant elements.

Acknowledgement. The author would like to thank the anonymous reviewers for constructive comments and helpful suggestions which led to the opportunity to revise and improve the paper.

References

- [1] W. T. Ang, A crack in an anisotropic layered material under the action of impact loading, *ASME Journal of Applied Mechanics* 55 (1988) 122-125.
- [2] J. R. Berger and A. Karageorghis, The method of fundamental solutions for heat conduction in layered materials, *International Journal for Numerical Methods in Engineering* 45 (1999) 1681-1694.
- [3] D. L. Clements, A crack in an anisotropic layered material, *Rozprawy Inżynierskie* 27 (1979) 171-180.
- [4] B. C. Lee and E. S. Kim, A simple and efficient method of analyzing mechanical behaviors of multi-layered orthotropic plates in rectangular shape, *Journal of Micromechanics and Microengineering* 9 (1999) 385-393.

- [5] Y. Benveniste and T. Miloh, Imperfect soft and stiff interfaces in two-dimensional elasticity, *Mechanics of Materials* 33 (2001) 309-323.
- [6] H. Fan and K. Y. Sze, On the decay of end effects in conduction phenomena: A sandwich strip with imperfect interfaces of low or high conductivity, *Mechanics of Materials* 33 (2001) 363-370.
- [7] W. T. Ang, K. K. Choo and H. Fan, A Green's function for steady-state two-dimensional isotropic heat conduction across a homogeneously imperfect interface, *Communications in Numerical Methods in Engineering* 20 (2004) 391-399.
- [8] H. Fan and G. F. Wang, Interaction between a screw dislocation and viscoelastic interfaces, *International Journal of Solids and Structures* 40 (2003) 763-776.
- [9] W. T. Ang and H. Fan, A hypersingular boundary integral method for quasi-static antiplane deformations of an elastic bimaterial with an imperfect and visco-elastic interface, *Engineering Computations* 21 (2004) 529-539.
- [10] C. A. Brebbia and D. Nardini, Dynamic analysis in solid mechanics by an alternative boundary element procedure. *International Journal of Soil Dynamics and Earthquake Engineering* 2 (1983) 228-233.
- [11] P. W. Partridge and C. A. Brebbia, The dual reciprocity boundary element method for the Helmholtz equation, In: Brebbia CA, Choudouet-Miranda A, editors, *Proceedings of the International Boundary Elements Symposium*, 1990, pp. 543-555.
- [12] F. Rizzo and D. J. A. Shippy, A method of solution for certain problems of transient heat conduction, *AIAA Journal* 8 (1970) 2004-2009.

- [13] D. L. Clements, *Boundary Value Problems Governed by Second Order Elliptic Systems*, Pitman, London, 1981.
- [14] J. T. Chen and H. K. Hong, Review of dual boundary element methods with emphasis on hypersingular integrals and divergent series, *Applied Mechanics Review* 52 (1999) 17-33.
- [15] W. T. Ang and D. L. Clements, Hypersingular integral equations for a thermoelastic problem of multiple planar cracks in an anisotropic medium, *Engineering Analysis with Boundary Elements* 23 (1999) 713-720.
- [16] Y. Zhang and S. Zhu, On the choice of interpolation functions used in the dual-reciprocity boundary-element method, *Engineering Analysis with Boundary Elements* 13 (1994) 387-396.
- [17] A. F. Moench and A. Ogata, A numerical inversion of the Laplace transform solution to radial dispersion in a porous medium, *Water Resources Research* 17 (1981) 250-252.
- [18] S. P. Zhu, P. Satravaha and X. P. Lu, Solving linear diffusion equations with the dual reciprocity method in Laplace space, *Engineering Analysis with Boundary Elements* 13 (1994) 1-10.
- [19] J. Sladek, V. Sladek and Ch. Zhang, A meshless local boundary integral method for dynamic antiplane shear crack problem in functionally graded materials, *Engineering Analysis with Boundary Elements* 29 (2005) 334-342.
- [20] H. Stehfest, Numerical inversion of the Laplace transform, *Communications of ACM* 13 (1970) 47-49 (see also p624).

- [21] W. T. Ang, A time-stepping dual-reciprocity boundary element method for anisotropic heat diffusion subject to specification of energy, *Applied Mathematics and Computation* 162 (2005) 661-678.
- [22] F. París and J. Cañas, *Boundary Element Method : Fundamentals and Applications*, Oxford University Press, Oxford 1997.